ISSN: 0975-8585

Research Journal of Pharmaceutical, Biological and Chemical Sciences

Estimating the Risk of Second Primary Cancer from Different Radiation Treatment Techniques Used in Prostate Radiotherapy.

Hala A. Soliman*.

Ionizing Radiation Metrology Lab., National Institute of Standards, Giza, Egypt.

Abstract

This work aimed at estimating the risk of second primary cancer for in-field and out-of-field organs for Prostate carcinoma treated by one-shot dose of 17.8 Gy using the linear-no-threshold and the competitive risk models. Carcinogenic estimates were calculated for the three treatment techniques by both of the risk models using published organ specific coefficients. The results confirmed that organs close to the target volume like Stomach has a developed second primary cancer risk ranged from 0.017% to 0.037% (for the three applied techniques). Distant organs; like Thyroid, showed an average risk of 0.00135%. Risks with intensity-modulated radiation therapy technique was generally higher for distant organs as a result of its increased monitor units demand. Estimating the developed second primary cancer for organs at risks using the dose-volume histogram analysis, reflects average risks of 0.5% and 1.12% for Bladder and Rectum; respectively, with a little difference between the applied techniques. The risks predicted in this study fitted best with the competitive risk model. Although considered low using this one-shot dose, it can be further reduced using different techniques of shielding.

Keywords: Second primary cancer; Risk models; TLD; IMRT; RA; 3D-CRT

https://doi.org/10.33887/rjpbcs/2019.10.5.18

Corresponding author

ISSN: 0975-8585

INTRODUCTION

Ionizing radiation has been recognized as a carcinogenic agent by the World Health Organization for many years [1,2]. The risk of second primary cancer (SPC) post radiation treatment has been known to be small but significantly increased compared with other treatment modalities [3]. The relationship between the incidence of this SPC and radiotherapy has been discovered since the evolution of the advanced external-beam radiotherapy for the treatment of cancer over the last several decades [4]. Abdel-Wahab et al, 2008 [5] defined SPC as a new tumor (neoplasm) which develops from normal tissue exposed to radiation and has histopathologic features different from the primary tumor ≥ 5 years after radiation treatment. Data from the Surveillance, Epidemiology and End Results (SEER) registry reflected the increased of total risk of developing SPC especially in the bladder and rectum, 5 years after diagnosis of prostate cancer. Some data indicated that men treated with external beam radiotherapy (EBRT) had higher risk than those who did not receive any radiation treatment [6]. There are many epidemiological investigations on the induction of secondary cancers following radiotherapy [7-15] but few of them relate the occurrence of it to the actual dose received by the irradiated organ and addressed the shape of the dose- response curve. Undesired secondary radiation, such as neutrons and leakage photons, can be generated during high-energy photon production in clinical linear accelerators and interact inside the patient body. Healthy tissues and OARs surrounding the target volume can absorb these scattered secondary radiations [16]. These out-of-field organs can be affected by these secondary radiations causing an increased risk of carcinogenesis [17]. Comparing to external beam radiotherapy; modern brachytherapy and proton treatments proposed to have a relatively lower risk of developing second primary cancer [18].

Although the three-dimensional conformal radiotherapy (3D-CRT) technique endeavor to minimize the volume of tissue surrounding the clinical target volume (CTV) that receive very low doses of radiation, the intensity modulated radiation therapy (IMRT) technique cause relatively large volumes of healthy tissues to be irradiated with these low doses. As the risks for stochastic effects associated with these techniques may not be the same [1,2], their treatment plans should be evaluated for these stochastic effects. Several suggestions recommend using the risk of cancer induction as a further criterion for the ranking of treatment plans along with the assessment of the deterministic effects [19-23]. Two main approaches to evaluate the risk of second primary cancers are in common use: an epidemiologic study and model-based risk estimation. In order to estimate the developed second primary cancer risk in any organ, standard radiation protection models are used especially in out-of-field regions of low doses. These models apply a single risk coefficient value (expressed in % per Sv) to the received equivalent dose of the organ [24].

Thus, the SPC risk linearly increases with the dose received. The linear no-threshold model (LNT) [25] is commonly convenient within the contexts of radiation protection. Linearity of the dose–response relationship for all cancers is assumed in this model, and the ICRP 99 indicates that the LNT hypothesis ‘‘remains a prudent basis for radiation protection at low doses and low dose rates” [25]. Other developed models look at individual organs/cancers allow for fractionation treatments used in radiotherapy.

Figure 1 shows the difference between risk calculation of the linear model and the competition model for both of single and fractionated dose irradiation. Repair of DNA damage results in less mutations and hence a reduced risk for cancers in the low dose range. Alternatively, the repair of DNA damage causes an increase of the risk for secondary cancers compared to the single dose case; noting that the dose-response curve seems to be dominated by the cellular survival, at the high dose range. The competition model is approximately linear at low doses, but then starts to fall at higher doses, consistent with the linear-quadratic function [26,27]. This CR model can also be applied in risk calculations to the nontargeted organs of inhomogeneous dose distributions using their dose-volume histograms. The intend of our work is to estimate the second primary cancer (SPC) risk for specific organs distal and close to the prostate target volume with a prescribed dose of one-shot of 17.8 Gy which is biologically equivalent to the usual prescribed dose of 76 Gy per 38 fractions with three different treatment techniques (IMRT, RA, and 3D CRT) by means of the linear-no-threshold (LNT) and the competitive risk (CR) model.

ISSN: 0975-8585

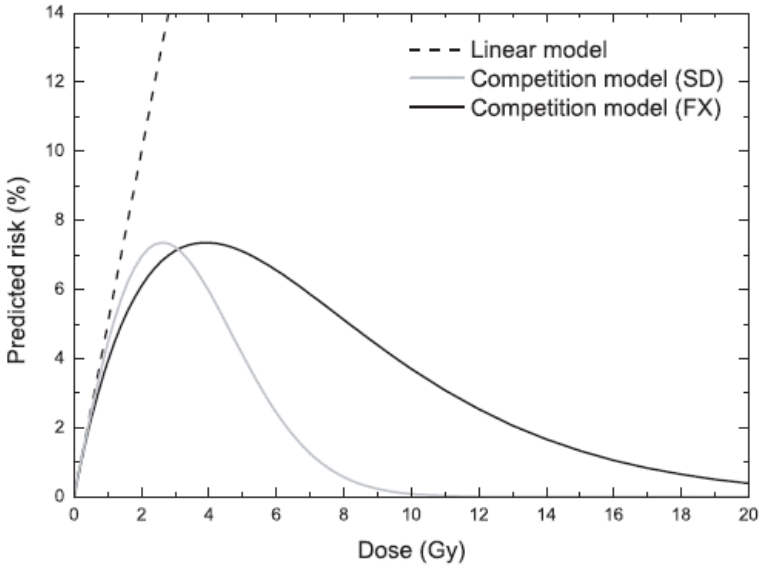

Figure 1. Estimation of risk calculated by the linear model (dashed line) and the competition model for single doses (grey solid line) and fractionated irradiations (black solid line). The linear model appears to be valid only for organ doses below 1 Gy. (α_1 = 0.05 Gy^{-1}, α_2 = 0.25 Gy^{-1}, α/β = 5 Gy) (Dasu et al, 2005) [27].

MATERIALS AND METHODS

An Anthropomorphic Alderson Rando phantom (Radiology Support Devices Inc., CA, USA) was delineated as a clinical prostate case (Figure 2). PTV (planning target volume) is defined as the prostate and seminal vesicles with a 0.5 cm posterior margin and 1 cm margin in the other directions. Also, organs at risks (OARs) such as Bladder and Rectum were delineated. The Rando phantom was Computed Tomography (CT) scanned, and three treatment plans for three treatment techniques of IMRT, RA, and 3D-CRT were generated from the Eclipse Treatment Planning Computer (TPS) (from Varian Medical Systems Inc., UK) version 11.0, simulating the prostate cancer case. Although out-of-field dosimetry in anthropomorphic phantoms is time consuming and restricted to treatment renovations [28], it is considered the "gold standard" in peripheral dose assessment [29].Thermoluminescent Detectors (TLDs) type TLD-700 (LiF; Mg, Ti) (Harshaw Chemical Company, Solon, OH) were implanted into the predrilled holes in the phantom slabs then irradiated on the linear accelerator (linac) Unique (Varian Medical Systems Inc., UK). The dosimeters are read by automatic RADOS RE-2000 TLD reader and the TLD analysis was performed by means of an established protocol accounts for system sensitivity, energy response, linearity and dosimeter fading. The TLD system uncertainty of dose calculation was 3.25%. The linac produces photon energy of 6 MV and the dose rate was up to 600 MU/minute. The prescribed photon dose was one-shot of 17.8 Gy which is biologically equivalent to 76 Gy/38 fractions, calculated with the linear quadratic model [30,31]. This photon dose was the same for the three different treatment plans and was used to reduce significantly the "beam-on" time to avoid the used linac to be energized for longer time. The total number of monitor units (Mus) required to deliver this photon dose were 6104, 6095, and 2976 for IMRT, RA, and 3D-CRT respectively. The IMRT plan used 9 equid-spaced coplanar fields while the 3D-CRT plan used 5 co-planar fields positioned in fan shape. The RA plan used 2 full arcs with posterior avoidance sector of 30° to 40° in the rectal region, with a collimator angle 30° and dose rate of 600 cGy/min.

All of the dosimetric data were obtained from TLD measurements for both of the normal organs within the CT planning volume (Bladder and Rectum), and the distant normal organs lying beyond the planning CT volume (Thyroid gland, Esophagus, Lung, Liver and Stomach). Dose-Volume Histogram (DVH) analysis provided dosimetric data for Bladder and Rectum only using the new commercially available Acuros XB (AXB) advanced dose calculation algorithm implemented in the Eclipse Treatment Planning System (TPS).The LNT model [25] is then used for estimating the SPC risk at low doses with a single risk coefficient (expressed in %/Sv) applied to the organ equivalent dose and also the modified CR model [7] which takes into consideration the effects of mutation induction at low doses, and cell killing at higher doses. This model can calculate the SPC risk for the inhomogeneous dose distributions within an organ using its Dose-Volume Histogram (DVH).

ISSN: 0975-8585

Figure (2) Anthropomorphic Alderson Rando phantom

In the present work, the SPC risk is estimated for any specific organ using the competitive risk model as described in Dasu et al. and Toma-Dasu et al. [26, 27] exploiting the following equation:

$$Effect(D) = \left(\alpha_1 D + \frac{\beta_1 D_2}{n}\right) x\, e - (\alpha_2 D + \frac{\beta_2 D^2}{n}) \quad (1)$$

Where D is the total dose delivered in *n* fractions as usual in clinical radiotherapy. Values of α_1 and β_1 are the linear and quadratic coefficients for induction of DNA mutations and α_2 and β_2 are linear and quadratic coefficients for cell kill [14]. For OARs (Bladder and Rectum), their dose-volume histograms were constructed by using differential volume data (based on the CT images of the organs in the RANDO phantom) planned in the Eclipse TPS. The whole risk effect for every organ was integrated over the entire organ DVH using the following equation [26]:

$$Effect(D) = \frac{\sum_i [(v_i \times Effect\ (D_i)]}{\sum_i v_i} \quad (2)$$

Where *Effect* (D_i) is the nonlinear dose response relationship of the CR model due to the dose D_i received by v_i volume of the organ delivered in *n* individual fractions.

The values of α/β, α_1, β_1, α_2 and β_2 for the bladder and rectum were taken from Takam et al, 2009 [4] and listed in table (1). We used the organ specific coefficient (α_1) listed in ICRP 103 [32] for different organs. It is 0.012Gy^{-1} for Lungs and Stomach, and 0.004 Gy^{-1} for Thyroid, Esophagus and Liver.

As heterogeneity has little effect on the cell survival parameter, and consequently on the estimated risk of second malignancy, the values of α_2 and α/β used in this work were 0.25 Gy^{-1}, and 5 Gy; respectively, based on Dasu & Toma-Dasu and Dasu et al. [26, 27].

Figure (1) shows the risk prediction of both the LNT and CR models for single irradiation doses (SD) and fractionated irradiations (FX) [27]. The predictions of the two models are fairly different, and the maximum of the CR model curves is ranged from 4 to approximately 5 Gy, which is consistent with the epidemiological studies [10]. The figure also shows a maximum risk level of about 7% using the general risk coefficient α_1 = 0.05 Gy^{-1}. The risk is proportional to the received dose by organs, and the linear model (LNT)

ISSN: 0975-8585

appears suitable for organ doses equal or below 1 Gy. At higher doses; cell kill becomes dominant and starts to constrain the effects of mutations.

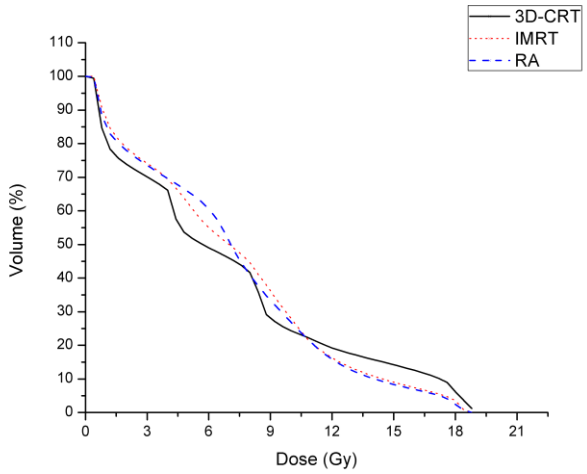

(a)

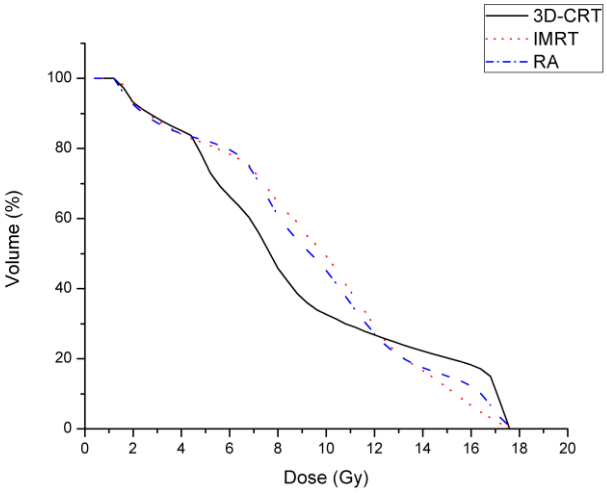

(b)

Figure (3) Dose-volume histograms for (a) Bladder and (b) for Rectum generated from the Eclipse treatment planning system

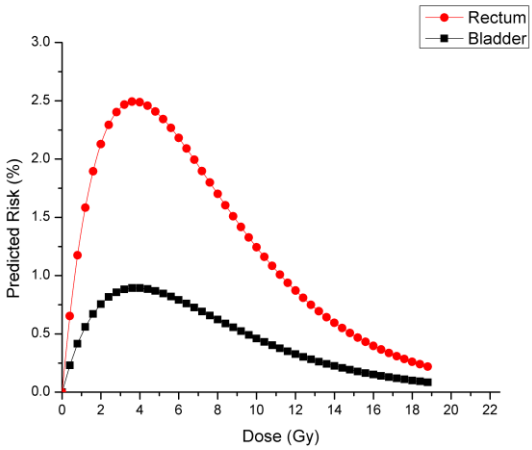

Figure (4) Predicted risk (%) of developing second primary cancer of OARs (rectum and bladder) using the CR model.

ISSN: 0975-8585

Table 1. Competitive risk model parameters used for estimation of second primary cancer risk following various radiation treatment techniques for prostate.

Organ	α/β	$\alpha 1$	$\beta 1$	$\alpha 2$	$\beta 2$
Rectum	5.4	0.017	0.003	0.25	0.046
Bladder	7.5	0.006	0.001	0.25	0.033

Table (2) Organ dose equivalent in mSv per unit photon Gy delivered to the isocenter from IMRT, RA, and 3D-CRT techniques.

Organ	IMRT	RA	3D-CRT
Thyroid	0.195	0.188	0.162
Esophagus	0.437	0.194	0.257
Lung	0.481	0.206	0.314
Liver	1.148	0.521	0.849
Stomach	1.738	0.798	1.268
Bladder	335	329	361
Rectum	371	351	391

Table (3) Calculated risks (in %) of second primary cancer using organ specific coefficients by employing the linear- no- threshold and competitive models resulting from prostate irradiation with 17.8 Gy by 6 MV photons for IMRT, RA, and 3D-CRT techniques.

Organ	IMRT		RA		3D-CRT	
	LNT model	CR model	LNT model	CR model	LNT model	CR model
Thyroid	1.39E-03	1.39E-03	1.34E-03	1.34E-03	1.34E-03	1.34E-03
Esophagus	3.11E-03	3.11E-03	1.38E-03	1.38E-03	1.83E-03	1.83E-03
Lung	1.03E-02	1.03E-02	4.40E-03	4.40E-03	6.71E-03	6.71E-03
Liver	8.21E-03	8.17E-03	3.72E-03	3.71E-03	6.06E-03	6.04E-03
Stomach	3.74E-02	3.71E-02	1.71E-02	1.70E-02	2.72E-02	2.71E-02
Bladder	7.15E+00	4.95E-01	6.95E+00	5.17E-01	7.99E+00	4.09E-01
Rectum	2.42E+01	6.30E-01	2.22E+01	7.81E-01	2.64E+01	4.98E-01

Table (2) shows the photon equivalent dose for each organ in mSv per photon gray delivered to the isocenter for the three applied treatment techniques (IMR, RA, and 3D-CRT). Results show a relationship between the peripheral photon doses and the distance from the therapeutic field, they decrease as increasing the distance from the edge of the field for all of the treatment techniques. The sources of these peripheral doses are scatter from the useful treatment beam within the patient, scatter from the collimating jaws, and photon leakage from the head of the used linac. The magnitude of these small out-of-field doses depend on some factors like: distance from the field edge, field size, beam energy and depth [33]. IMRT technique shows the higher scattered photon doses as a whole and at large distances from the isocenter due to the collimator scatter and head leakage. Lung, Esophagus, and Thyroid (at distances more than 40 cm from isocenter) have higher peripheral doses when using the IMRT technique than the 3D-CRT technique. The ratio factor was 1.53, 1.7, and 1.2 for Lung, Esophagus, and Thyroid; respectively. This was attributed to the head leakage scatter component results from field modulation of the IMRT technique and using more monitor units comparing with the unmodulated field as in the 3D-CRT technique [34-36].

Stomach and Liver organs far from the field isocenter by a distance of 32 cm and 31.5 cm respectively as previously measured and estimated by Howell et al, 2006 [33]. The peripheral photon doses to these organs are greater from IMRT than 3D-CRT by a factor of ~1.4. These doses are distributed from scatter from inside the patient and from head leakage [37]. The doses to the Bladder and Rectum (corrected for supralinearity) are all greater for the 3D-CRT technique than the IMRT technique as a result of the beam intensity modulation,

in full dose coverage of the planning target volume while reducing the dose to organs at risk. The RA technique resulted in an overall decrease in the out-of-field doses to many organs compared to the other two techniques (except for the Thyroid gland); also, the best one in minimizing doses to OARs.

Table (3) shows the calculated risk (in %) of developing SPC to some distant organs and normal critical organs for a full prostate radiation treatment with the three employed techniques (IMRT, RA, and 3D-CRT) by a one-shot dose of 17.8Gy (per one fraction) which is equivalent to 76 Gy per 38 fractions using 6 MV beam from the Unique linac. The organs SPC risks are calculated by equation (1) using their organ specific coefficient and the received dose equivalents. The predicted risks of SPC shown in the "LNT model" column of this table is mentioned to the risk of SPC calculated using the linear term of the CR model which represents the effect of DNA mutations only.

The "CR model" column shows the estimated risk of SPC using the whole equation (including both of the linear and quadratic terms). The photon dose equivalents were derived assuming uniform dose distribution in each organ. The risk of developing SPC in each affected organ increases proportionally with dose. In table (3), organs close to the target volume like stomach has a risk of developing SPC (0.017-0.037 %) greater than that any other distant organ (e.g. 0.0013-0.0014 for thyroid). Generally, the risk of developing SPC increases proportionally with dose for the two applied risk models until the radiation dose to the organs increases to levels where cell kill of already mutated cells is attained. Hence, the difference between the risk of SPC calculated with the linear term only and with the full equation can be noticed, e.g. in the case of critical organs (Bladder and Rectum). IMRT technique shows the highest carcinogenic risk for the distant organs because of the higher monitor units demand for it to expose the target volume with the same prescribed dose (17.8 Gy) as the other two techniques. The increase in monitor units increases the head leakage scatter component of the used linac and consequently more scattered radiation doses to these organs.

In the present study setting, the Mus demand for the IMRT technique (6104) was 2 times that of the 3D-CRT technique (2976), and hence its associated risk was generally higher; for example, the risk to the Esophagus organ using the IMRT technique was 1.7 times higher than that associated with the 3D-CRT technique. Organs at risk surrounding the target volume, such as Bladder and Rectum have the highest risk of developing cancer. The LNT model overestimated the risk (7-8% for Bladder and 22-26% for Rectum) than that of the CR model (0.41-0.52% for Bladder and 0.5-0.6% for Rectum). The observed differences in risk estimation by the two models are results of employing the quadratic term (the second term of the equation) of the CR model which represents cell kill and reduction in survival of transformed cells causing decrease in the total risk of mutations. Bladder and Rectum are in-field organs and within the DVH volume. Figure 3 (a) and (b) shows the dose-volume histograms for Bladder and for Rectum generated from the Eclipse TPS and their dose distribution as a result of the treatment plans of the applied treatment techniques.

We used the DVH dosimetric data of these organs and employed it in the calculation of the SPC risk estimation (for the IMRT, RA, and 3D-CRT techniques) by means of equations (2) and (3) of the CR model. Figure 4 reveals the predicted risk (%) of SPC of the Bladder and Rectum in relation to dose (Gy) calculated using equation (2) and shows their dose-response relationship. SPC risks were estimated using the α/β ratio of 7.5 for the Bladder and 5.4 for the Rectum. According to the competitive risk model, the risk increases with dose reaching a maximum around 3-5 Gy upon which mutated cell survival is likely. Further increase in the dose, decreases risk and radiation kill dominates causing a reduction in the survival of transformed cells.

The estimated risks of developing SPC were 0.49, 0.50, and 0.52 for Bladder and 1.11, 1.11, and 1.15 for Rectum for the IMRT, RA, and 3D-CRT techniques respectively.

Estimating the developed SPC for OARs using the DVH analysis, result in average risks of 0.50% and 1.12% for Bladder and Rectum respectively, with a little difference between the applied techniques. On the contrary, when using the organ-averaged equivalent doses using the TLD detectors, their average SPC risks from the three applied techniques were 0.47% and 0.64% for Bladder and Rectum respectively. Results with respect to the increased risk of SPC development in OARs when using their DVH data propose that it is important to include all the particulars of the irradiation pattern inside the organ. Therefore, the use of a nonlinear model and the full dose distribution within the organ are anticipated to give better cancer risk estimations. Risk of SPC development in distant organs (organs far from the treatment volume) can be estimated using their organ-averaged doses measured by TLDs where their DVHs are difficult to reconstruct.

IMRT technique greatly reduces dose to nearby organs (OARs) but yields higher doses to distant organs because of the great number of monitor units demand compared with using the same dose from unmodulated fields. Thus, increasing the magnitude of scattered radiation and head leakage from the used linac, and consequently the resultant carcinogenic risk compared to the other techniques.

CONCLUSION

Our results show that a dose level was found between in-field organs and out-of-field organs (distant organs), and its magnitude decreases as increasing the distance from the target volume.

RA and IMRT techniques minimize dose to OARs compared to the 3D-CRT technique. Although integral dose to healthy tissues within the DVH volume (OARs) is relatively unchanged by IMRT, it has been reported to increase to distant organs and hence its carcinogenic risk. IMRT may double the risk of secondary cancers, compared with conformal radiotherapy, because of its large number of monitor units demand; increasing the dose outside the boundary of the primary collimator and irradiating a large volume of normal tissues to low doses. The risks predicted in our study fitted well with the CR model for both of low and high doses.

Although these predicted risks considered low (using a prescribed one-shot dose of 17.8 Gy from 6 MV photon beams), it is considered by practitioners as a compromised charge of success for the used advanced techniques in prostate radiotherapy. However, risks of developing SPC can be reduced by providing radiation protective measures for the patient during irradiation by using different techniques of shielding to reduce dose from secondary radiations.

ACKNOWLEDGMENTS

The author thanks sincerely Dr. Ranya Moussa and Dr. Maha Kamaleldien from the Radiation Physics Department, Faculty of Medicine, Cairo University for their patience and kind assistance in carrying out the experimental work.

REFERENCES

[1] El Ghissassi F, Baan R, Straif K, Grosse Y, Secretan B, Bouvard V, Benbrahim-Tallaa L, Guha N, Freeman C, Galichet L and Cogliano v. "A review of human carcinogens part D, radiation. Lancet Oncol., 2009; 10 (8):751–752. [PubMed: 19655431]

[2] UNSCEAR. Annex A, Epidemiological studies of radiation and cancer. In: UNSCEAR Report 2006, Effects of Ionizing Radiation, 2006; Vol. I. United Nations Office; Vienna.

[3] Dörr W and Herrmann T. Second tumors after oncologic treatment Strahlenther, Onkol., 2008; 184: 67–72.

[4] Takam R, Bezak E and Yeoh EE. Risk of second primary cancer following prostate cancer radiotherapy: DVH analysis using the competitive risk model, Phys Med Biol, 2009; 54(3), 611–625.

[5] Abdel-wahab M. and Reis IM, Hamilton K., Second primary cancer after radiotherapy for prostate cancer-a SEER analysis of brachytherapy versus external beam radiotherapy, International Journal of Radiation oncology Biology Physics, 2008; 72, 58-68.

[6] Moon K, Stukenborg G J, Keim J and Theodorescu D., Cancer incidence after localized therapy for prostate cancer, Cancer, 2006; 107, 991–998.

[7] Gray LH, William & Wilkins., Radiation biology and cancer. In: Cellular radiation biology: a symposium considering radiation effects in the cell and possible implications for cancer therapy, Baltimore, 1965: 8–25.

[8] Upton AC., Radiobiological effects of low doses. Implications for radiological protection, Radiat Res, 1977; 71:51-74.

[9] Mole RH., Dose-response relationships. In: Boice JD, Fraumeni Jr JF, editors. Radiation carcinogenesis: epidemiology and biological significance (1984). New York: Raven Press: 403-20.

[10] Dörr W and Herrmann T., Cancer induction by radiotherapy: dose dependence and spatial relationship to irradiated volume, J Radiol Prot, 2002; 22: A117-21.

[11] Tucker MA, Jones PH, Boice Jr JD, Robison LL, Stone BJ, Stovall M and et al., Therapeutic radiation at a young age is 834 A. Dasu & I. Toma-Das¸u linked to secondary thyroid cancer, The Late Effects Study Group, Cancer Res, 1991; 51: 2885-8.

[12] Joiner MC, Marples B, Lambin P, Short SC and Turesson I., Low-dose hypersensitivity: current status and possible mechanisms, Int J Radiat Oncol Biol Phys, 2001; 49: 379-89.

[13] Dasu¸ A, Toma-Das¸u I and Fowler JF., Should single or distributed parameters be used to explain the steepness of tumor control probability curves? Phys Med Biol, 2003; 48: 387-97.

[14] UNSCEAR 1993 Report. United Nations Scientific Committee on the Effects of Atomic Radiation, Sources and effects of ionizing radiation. New York: United Nations; 1993.

[15] ICRP. ICRP Publication 60: 1990 Recommendations of the International Commission on Radiological Protection. Annals of the ICRP, 1991; 21: 1-202.

[16] Becker J, Brunckhorst E and Schmidt R., Photo-neutron production of a Siemens Primus linear accelerator studied by Monte Carlo methods and a paired magnesium and boron coated magnesium ionization chamber system, Phys Med Biol, 2007; 52: 6375–87

[17] Eva Bezak, Rundgham Takam, Eric Yeoh, Loredana G, and Marcu., The risk of second primary cancers due to peripheral photon and neutron doses received during prostate cancer external beam radiation therapy, Physica Medica, 2017; 42: 253-258

[18] Murray L, Henry A, Hoskin P, Siebert FA, Venselaar J. ESTRO BPgotG., Second primary cancers after radiation for prostate cancer: a review of data from planning studies. Radiat Oncol, 2013; 8:172.

[19] Bhatia S, Robison LL, Oberlin O, Greenberg M, Bunin G, Fossati-Bellani F., Breast cancer and other second neoplasms after childhood Hodgkin's disease, N Engl J Med, 1996; 334: 745-51.

[20] Epstein R, Hanham I. and Dale R., Radiotherapy-induced second cancers: are we doing enough to protect young patients? Eur J Cancer, 1997; 33: 526-30.

[21] Schneider U, Lomax A and Lombriser N., Comparative risk assessment of secondary cancer incidence after treatment of Hodgkin's disease with photon and proton radiation, Radiat Res, 2000; 154: 382-8.

[22] Lindsay KA, Wheldon EG, Deehan C and Wheldon TE., Radiation carcinogenesis modelling for risk of treatmentrelated second tumours following radiotherapy, Br J Radiol, 2001; 74: 529-36.

[23] Miralbell R, Lomax A, Cella L and Schneider U., Potential reduction of the incidence of radiation-induced second cancers by using proton beams in the treatment of pediatric tumors, Int J Radiat Oncol Biol Phys, 2002; 54: 824-9.

[24] National Research Council, Health risks from exposure to low levels of ionizing radiation: BEIR VII Phase 2. Washington, DC: The National Academies Press; 2006.

[25] ICRP 99, Low-dose Extrapolation of Radiation-related Cancer Risk. ICRP Publication 99. Ann ICRP; 2005,35

[26] Dasu A and Toma-Dasu I., Dose-effect models for risk-relationship to cell survival parameters, Acta Oncol, 2005; 44, 829–35.

[27] Dasu A, Toma-Dasu I, Olofsson J and Karlsson M., The use of risk estimation models for the induction of secondary cancers following radiotherapy 2005; Acta oncol, 44: 339–47.

[28] Roger Harrison, Out-of-field doses in radiotherapy: Input to epidemiological studies and dose-risk models, Physica Medica, 2017; 42: 239-246.

[29] Saveta Miljanic, logr Bessieres, Jean -Marc Bordy, Francesco d'Errico, Angela Di Fulvio, Damian Kabat, Zeljka Knezevic, Pawel Olko, Liliana Stolarczyk, Luigi Tana and Roger Harrison, Clinical simulations of prostate radiotherapy using BOMAB-like phantoms: Results for photons, Radiation Measurments, 2013; 57: 35-47.

[30] J. F. Fowler, The linear-quadratic formula and progress in fractionated radiotherapy, *Br. J. Radiol.,* 1989; 62: 679-694.

[31] Brenner, D. J., Hlatky, L. R., Hahnfeldt, P. J., Huang, Y. and Sachs, R. K., The Linear-Quadratic Model and Most Other Common Radiobiological Models Result in Similar Predictions of Time-Dose Relationships, *Radiat. Res,* 1998 150: 83-91.

[32] ICRP publication 103. The 2007 Recommendations of the International Commission on Radiological Protection. Ann ICRP, 2007; 37: 1–332.

[33] Howell RM, Hertel NE, Wang ZL, Hutchinson J and Fullerton GD., Calculation of effective dose from measurements of secondary neutron spectra and scattered photon dose from dynamic MLC IMRT for 6 MV, 15 MV, and 18 MV beam energies, Med Phys, 2006; 33: 360–8. [PubMed: 16532941]

[34] Aoyama H, Westerly DC, Mackie TR and et al., Integral radiation dose to normal structures with conformal external beam radiation, Int J Radiat Oncol Biol Phys, 2006; 64: 962–967.

[35] Mackie T, Kissick M, Jeraj R and et al., Integral dose in external beam photon radiotherapy [Abstract], Med Phys, 2004; 31: 1271.

[36] Della Biancia C., Hunt M. and Amols HA., A comparison of the integral dose from 3D conformal and IMRT techniques in the treatment of prostate cancer [Abstract], Med Phys, 2002; 29: 1216.

[37] American Association of Physicists on Medicine, "Fetal dose from radiotherapy with photon beams: Report of AAPM Radiation Therapy Committee Task Group No. 36," Med. Phys. 1995; 221: 63–82.